SULFURIC ACID BAKING OF PARTIALLY DECOMPOSED RIRUWAI ZIRCON SAND: PROCESS OPTIMIZATION USING RESPONSE SURFACE METHODOLOGY TOWARD FOUNDRY SPECIFICATIONS

Mohammed, A.*, Kareem, S.A. and Saddiq, H.A.

Department of Chemical Engineering, Modibbo Adama University Yola, Adamawa State, Nigeria

*Corresponding email: amajalingo@mau.edu.ng

ABSTRACT

Riruwai zircon sand from Nigeria contains exceptionally high concentrations of uranium and thorium (>26,000 ppm), making conventional fine milling undesirable because of the associated generation of radioactive dust. This study investigates sulfuric acid baking as the second stage of a two-stage chemical beneficiation process for upgrading partially decomposed Riruwai zircon sand toward foundry specifications without fine milling. The starting material, obtained from a previous partial decomposition treatment, contained sodium zirconate (Na_2ZrO_3) as an intermediate phase together with residual zircon and associated impurities. Response Surface Methodology based on a Central Composite Design was employed to optimize the sulfuric acid baking process by evaluating the effects of temperature, baking time, and solid-to-liquid ratio on iron and combined uranium-thorium (U+Th) removal. The solid-to-liquid ratio was identified as the most influential process variable for both responses, followed by temperature. Numerical optimization predicted optimum conditions of 291 °C, 120 min, and a solid-to-liquid ratio of 1.5, which were validated experimentally. Under these conditions, the U+Th concentration decreased from 17,200 ppm in the partially decomposed zircon to 252 ppm, satisfying the foundry specification of <500 ppm, while Fe_2O_3 was reduced from 2.34% to 0.82%, remaining above the required limit of 0.30%. The $ZrO_2 + HfO_2$ content increased from 58.37% to 67.76%, exceeding the minimum requirement of 65%. X-ray diffraction confirmed the complete removal of sodium zirconate and monazite, with zircon increasing to 94% as the dominant mineral phase. The study demonstrates that sulfuric acid baking following partial decomposition provides an effective route for substantially reducing radionuclide concentrations and upgrading highly radioactive Riruwai zircon toward foundry specifications without the need for fine milling, thereby reducing potential health risks associated with radioactive dust generation.

Keywords: Riruwai zircon, Acid baking, Foundry sand, Metamictization, Response surface methodology

1 INTRODUCTION

Zircon or zirconium silicate ($ZrSiO_4$) is a critical raw material for industrial applications, including foundries, ceramics, and refractories [1, 2]. The mineral offers high refractoriness, low thermal expansion, and excellent chemical stability. For foundry applications, zircon sand must satisfy both chemical and physical specifications. Among the chemical requirements, the most critical are combined uranium and thorium (U + Th) contents below 500 ppm, iron oxide (Fe_2O_3) below 0.30 wt.%, and combined zirconia and hafnia ($ZrO_2 + HfO_2$) above 65 wt.% [3]. In addition to these chemical requirements, the performance of zircon sand in foundry applications is also influenced by its physical properties, particularly grain characteristics and thermal behaviour [4]. Zircon is commonly found in heavy mineral sand deposits, where it accumulates through natural processes such as water

and wind action. It can also be recovered from tailings generated during the processing of mineral ores like tin (cassiterite) and gold. In Nigeria, zircon sand is predominantly obtained as a by-product from the processing of cassiterite tailings [5]. Nigerian zircon obtained from cassiterite processing typically contains high levels of impurities, including iron, cassiterite, uranium, and thorium among others [6]. Elevated radionuclide levels can cause metamictization, a radiation-induced amorphization of the zircon crystal lattice [7, 8]. The process degrades physical properties but increases chemical reactivity in damaged regions. Uranium and thorium along with other impurities can become embedded within the lattice of metamict zircon, making them difficult to remove without complete structure decomposition [7, 9]. Physical beneficiation alone cannot remove lattice-bound impurities [3], necessitating the need for chemical treatments to remove impurities. A variety of chemical treatment approaches are available, yielding a broad range of end products. The most widely applied include alkali fusion, which fully decomposes zircon to produce zirconia (ZrO_2), and acid-based treatments, which involve either high-temperature acid baking or aqueous acid leaching, typically using sulfuric. In alkali fusion, zircon is reacted with excess sodium hydroxide at temperatures above 600 °C, followed by multistep processing to isolate zirconia [10]. While this method is cost effective, scalable, and efficient in removing both surface and lattice-bound impurities including radioactive elements, it results in the complete breakdown of zircon into zirconia, which limits its suitability for applications that require intact zircon structure [11]. Acid treatments tend to be more selective, effectively removing surface impurities while largely preserving the zircon crystal structure. Nevertheless, these methods are often insufficient for eliminating impurities embedded within the lattice [9]. Fine milling is commonly used to increase the reactivity of zircon by reducing particle size and exposing surface-bound impurities. However, for Riruwai zircon, fine milling presents significant challenges. Zircon has a hardness of 7.5 Mohs, which causes rapid equipment wear and high energy consumption during milling [3]. More critically, the high uranium and thorium content (>26,000 ppm) [12] means that milling generates fine radioactive dust. Inhalation of this dust poses serious health risks to workers, including radiation exposure and the potential for long-term lung damage [3, 6]. Regulatory limits for airborne radioactive particles require extensive dust control measures, adding further costs. For these reasons, any purification process that avoids fine milling offers substantial safety and economic advantages. The present process exploits the natural cracks and fissures present in metamict zircon as pathways for acid penetration, eliminating the need for milling to achieve impurity removal. In our previous study, a partial decomposition method was developed to serve as a first of a two-stage treatment process [12]. Optimized conditions for the partial decomposition stage were sub-stoichiometric NaOH (0.8× stoichiometric amount required) a temperature of 409^{o}C and time 49 minutes. This treatment reduced U+Th from 26,200 ppm to 17,200 ppm and formed 18% sodium zirconate (Na_2ZrO_3) while preserving the bulk zircon structure. The product also contained 77% residual zircon, 3% cassiterite, 1% monazite, and 1% quartz. The present study focuses exclusively on the second stage in which acid baking is used for impurity removal. Acid baking is an established technique for decomposing refractory minerals. The material is heated with concentrated sulfuric acid and some impurities are converted into water-soluble sulfates [13, 14]. When applied to sodium zirconate, sulfuric acid converts it to soluble zirconium sulfate while promoting the dissolution of impurity-bearing phases [15]. However, the influence of sulfuric acid baking conditions on the purification of partially decomposed Riruwai zircon has not been systematically investigated. Accordingly, this study employed Response Surface Methodology based on a Central Composite Design to optimize the sulfuric acid baking process by evaluating the effects of temperature, baking time and solid-to-liquid ratio on the removal of Fe and U+Th from partially decomposed Riruwai zircon sand.

2 MATERIALS AND METHODS

2.1 Starting Material

The starting material was partially decomposed Riruwai zircon sand with mean particle size 212 µm. It was prepared under optimal conditions established in previous work [12]. Table 1 presents the characteristics of this material.

Table 1. Characteristics of partially decomposed Riruwai zircon sand

Parameter	Value (%)
Zircon	77
Sodium zirconate (Na_2ZrO_3)	18
Cassiterite (SnO_2)	3
Monazite	1
Quartz	1
ZrO_2+ HfO_2	58.37
Fe_2O_3	2.34
U_3O_8 + ThO_2	1.72

2.2 Experimental Design

Response Surface Methodology with Central Composite Design (RSM-CCD) was employed. The three independent factors and their ranges were based on preliminary studies and literature [13,14]: The solid-to-liquid (S/L) ratio is the mass of zircon sand divided by the mass of concentrated sulfuric acid. For a fixed sand mass of 20 g, S/L = 1.5 corresponds to 13.3g acid (higher acid availability). S/L = 3.0 corresponds to 6.7 g acid (lower acid availability). Thus, lower S/L values indicate higher acid availability; this definition is consistent with previous work [12]. The responses measured were residual Fe_2O_3 (%) and residual U+Th (ppm), both were determined by XRF. A full factorial rotatable CCD was used for the study, it comprised 20 experimental runs: 8 factorial points, 6 axial points, and 6 center points. Table 2 shows conditions for Sulfuric Acid Baking.

Table 1. Conditions for Sulfuric Acid Baking

		Levels		
Factor	Symbol	Low (-1)	Center (0)	High (+1)
Temperature (ºC)	A	200	250	300
Time (min)	B	60	90	120
Solid/Liquid ratio	C	1.50	2.25	3.00

2.3 Acid Baking Procedure

For each run, 20g of partially decomposed Riruwai zircon sand was mixed with concentrated H_2SO_4 at the specified S/L ratio. The mixture was placed in a porcelain crucible and homogenized with a glass rod. The crucible was placed in a preheated muffle furnace at the set temperature for the specified duration.After heating, the crucible was removed and allowed to cool. The baked mass was washed with distilled water maintained below 50ºC. This temperature prevents silica gel formation (which occurs above 50ºC) and minimizes thorium hydrolysis [10]. Washing continued until the decanted wash water reached neutral pH (measured with a calibrated pH meter). The residue was dried at 105ºC to constant weight and stored in airtight containers.

2.4 Analytical Methods

Chemical composition was determined using a Thermo Scientific ARL QUANT'X EDXRF spectrometer. Samples were dried at 105ºC for 2 hours, then milled to a fine powder (approximately <75 μm). Approximately 5 g of each sample was placed in a sample cup with a thin film support. Montana Soil SRM 2710 was used as the standard reference material for calibration. Analysis was performed under vacuum for 10 minutes per sample. Mineral phase identification was performed using a Panalytical Empyrean diffractometer with Cu Kα radiation (λ = 1.5406 Å). Phase identification was carried out using X'Pert HighScore Plus software with the ICDD PDF-2 database (Gates-Rector and Blanton, 2019), while semi-quantitative phase analysis was based on the Reference Intensity Ratio (RIR) method [16].

2.5 Statistical Analysis

ANOVA was performed at a 95% confidence level ($p < 0.05$) [17]. Model adequacy was assessed using R^2, adjusted R^2, predicted R^2, coefficient of variation (CV), and adequate precision.

Numerical optimization used the Derringer-Suich desirability function. Validation experiments were conducted in triplicate and results reported as mean ± standard deviation [18].

3 RESULTS AND DISCUSSION

3.1 Model Development and ANOVA

The quadratic model was selected for both responses. Selection was based on sequential sum of squares and lack-of-fit tests. ANOVA results are presented in Tables 3and 4.

Table 2. ANOVA for Residual Fe after Acid Baking

Source	Sum of Squares	df	Mean Square	F Value	p-value Prob > F	
Model	0.734	9	0.082	26.858	< 0.0001	Significant
A-Temperature	0.110	1	0.110	36.089	0.0001	
B-Time	0.029	1	0.029	9.691	0.0110	
C-Solid/Liquid Ratio	0.449	1	0.449	147.700	< 0.0001	
AB	0.000	1	0.000	0.016	0.9005	
AC	0.014	1	0.014	4.757	0.0542	
BC	0.000	1	0.000	0.148	0.7084	
A^2	0.093	1	0.093	30.669	0.0002	
B^2	0.000	1	0.000	0.003	0.9541	
C^2	0.027	1	0.027	8.910	0.0137	
Lack of Fit	0.017	5	0.003	1.322	0.3834	not significant
Pure Error	0.013	5	0.003			
C.V. %	4.772					
R-Squared		0.9603				
Adj R-Squared		0.9245				
Pred R-Squared		0.8028				
Adeq Precision		20.6685				

Table 3 shows that the model is highly significant, with a p-value well below the 0.05 threshold. Temperature (p = 0.0001, F = 36.089) has a highly significant effect on iron removal, indicating that changes in temperature strongly influence the rate or extent of the sulfuric acid baking process. Higher temperatures likely enhance the dissolution of iron-bearing impurities by accelerating reaction kinetics. Time (p = 0.0110, F = 9.691) is also a significant factor, though its impact is less pronounced than that of temperature. The solid-to-liquid ratio (p < 0.0001, F = 147.700) is the most significant factor, as reflected by its high F-value and very low p-value [17].Interactions between temperature and time (AB) (p = 0.9005) and time and the solid-to-liquid ratio (BC) (p = 0.7084) are not significant, meaning that these factor combinations do not have a meaningful combined effect on iron removal beyond their individual impacts. However, the interaction between temperature and the solid-to-liquid ratio (AC) is borderline significant (p = 0.0542), suggesting that the effect of temperature on iron removal may depend on the solid-to-liquid ratio. Optimizing one without considering the other could lead to suboptimal results. The quadratic term for temperature (A^2) (p = 0.0002, F = 30.669) is highly significant, indicating a non-linear relationship between temperature and iron removal. Similarly, the quadratic term for the solid-to-liquid ratio (C^2) (p = 0.0137, F = 8.910) is also significant, pointing to a non-linear effect, with a possible optimal ratio beyond which iron removal becomes less efficient. In contrast, the quadratic term for time (B^2) (p = 0.9541) is not significant, indicating that the effect of time on iron removal is likely linear, without a clear optimal point within the experimental range. Based on the F-values obtained, the order of significance of the model terms was C > A> A^2> B > C^2> AC > BC > AB > B^2. The model shows good statistical performance, with a non-significant lack of fit with a p-value of 0.3834 and an R-squared value of 0.9603, indicating it explains 96.03% of the variability in iron removal. The adjusted R-squared (0.9245) and predicted R-squared (0.8028) are in good agreement, while the adequate precision value (20.6685) exceeds the threshold of 4, making the model suitable for optimization. Additionally, the coefficient of variance (CV) is 4.772, below the acceptable limit, confirming the model's reliability [17, 18]. The final regression equation, expressed in terms of coded factors, for predicting the residual Fe is presented in Equation (1).

$$\text{Fe (residual)} = 1.13 - 0.090A - 0.046B + 0.18C + 0.043AC + 0.080A^2 - 0.043C^2 \quad (1)$$

Similarly, the ANOVA results for the removal of U+Th from zircon sand using sulfuric acid baking is presented in Table 4. The model is also significant, as indicated by the F-value (32.85) and the extremely low p-value. Temperature is a highly significant factor for the removal of U+Th ($p < 0.0001$, $F = 61.48$). This could be due to accelerated reaction kinetics at elevated temperatures, which promote the dissolution of uranium and thorium compounds [10]. The effect of time on the baking process is also significant ($p = 0.0102$, $F = 9.96$), though less pronounced than temperature. The zircon/acid ratio, i.e, solid/liquid is seen as the most significant factor, as indicated by the highest F-value (16651). Suggesting the availability of sulfuric acid relative to the zircon sand mass is crucial for the effective leaching of U + Th. A higher acid availability likely facilitates more efficient contact between the acid and impurities, leading to better removal [13].

Table 3. ANOVA for Residual U+Th after Acid Baking

Source	Sum of Squares	df	Mean Square	F Value	p-value Prob > F	
Model	52838.06	9	5870.90	32.85	< 0.0001	Significant
A-Temperature	10987.10	1	10987.10	61.48	< 0.0001	
B-Time	1779.85	1	1779.85	9.96	0.0102	
C-Solid/Liquid Ratio	29758.07	1	29758.07	166.51	< 0.0001	
AB	28.13	1	28.13	0.16	0.6999	
AC	435.13	1	435.13	2.43	0.1497	
BC	3.13	1	3.13	0.02	0.8974	
A^2	5541.38	1	5541.38	31.01	0.0002	
B^2	236.70	1	236.70	1.32	0.2766	
C^2	3183.31	1	3183.31	17.81	0.0018	
Lack of Fit	1319.14	5	263.83	2.82	0.1400	not significant
Pure Error	468.00	5	93.60			
C.V. %	3.88					
R-Squared			0.9673			
Adj R-Squared			0.9378			
Pred R-Squared			0.8043			
Adeq Precision			23.6656			

The interactions between temperature and time (AB), temperature and solid/liquid ratio (AC) and time and solid/liquid ratio (BC), are not significant. The quadratic terms for temperature ($p = 0.0002$, $F = 31.01$) and solid/liquid ratio ($p = 0.0018$, $F = 17.81$) are highly significant, indicating a non-linear relationship between them and U+Th removal. This suggests that there may be an optimal temperature and solid/liquid ratio for the removal process, beyond which increasing them may not significantly enhance removal or could even be detrimental [10]. The quadratic term for time, however, is not significant, indicating that time has a more linear effect on the removal of U + Th. Based on the F-values obtained, the order of significance of the model terms was $C > A > A^2 > C^2 > B > AC > B^2 > AB > BC$. The model's lack of fit, R-squared (0.9603), adjusted R-squared (0.9245), predicted R-squared (0.8028), adequate precision (20.6685) and coefficient of variance (CV) all show the suitability and reliability of the model to predict U+Th removal from partially decomposed zircon sand using sulfuric acid baking [17, 18]. The final regression equation, expressed in terms of coded factors, for predicting the residual U + Th is presented in Equation (2).

$$\text{U} + \text{Th (residual)} = 338.19 - 28.36A - 11.42B + 46.68C + 19.61A^2 - 14.86C^2 \qquad (2)$$

Figures 1A-1C show the three-dimensional response surfaces for residual Fe as a function of temperature, time, and solid-to-liquid (S/L) ratio, while Figures 2A-2C present the corresponding response surfaces for residual U + Th. The response surfaces indicate that the residual Fe decreased markedly at temperatures between 250 and 275°C. This behaviour is attributed to improved sulphation of iron-bearing phases, enhancing their dissolution during subsequent aqueous leaching [13]. At an S/L ratio of 1.5, Fe removal reached approximately 92%. Similarly, residual U + Th decreased progressively with increasing temperature and benefited from the maximum baking time of 120 min. At an S/L ratio of 1.5, the residual U + Th concentration fell below 300 ppm, indicating enhanced removal of radioactive impurities under conditions of higher acid availability [10].

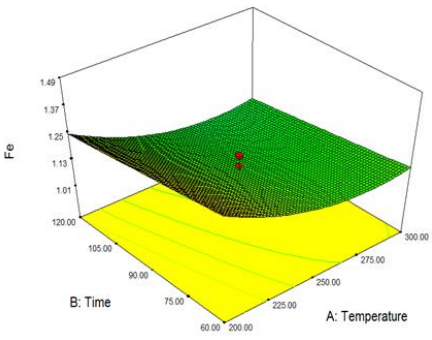

Figure 1A. Combined effect of time and temperature temperature on residual Fe after acid baking

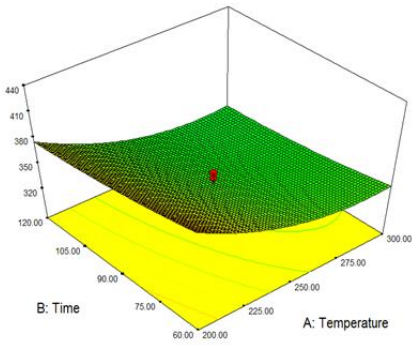

Figure 1B. Combined effect of time and on residual U + Th after acid baking

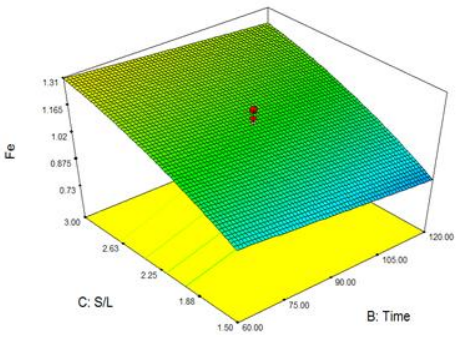

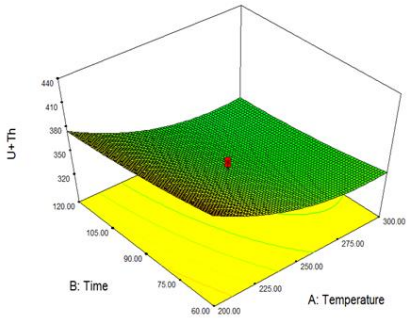

Figure 2C. Combined effect of S/L and Figure 2A.Combined effect of time and temperature time on residual Fe after acid bakingon residual U + Th after acid baking

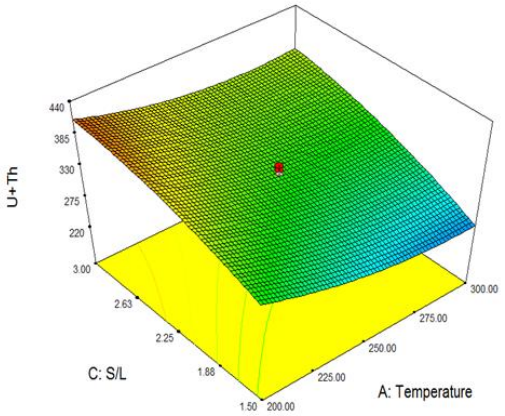

Figure 2B. Combined effect of S/L and temperature on residual U + Th after acid baking

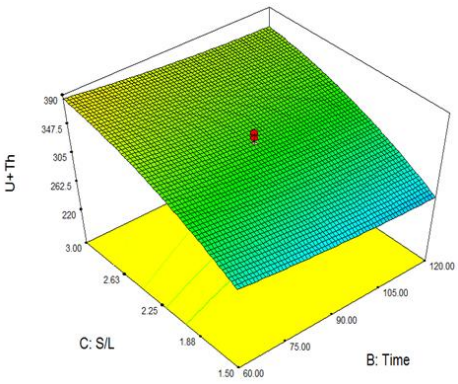

Figure 2C. Combined effect of S/L and time on residual U + Th after acid baking

3.2 Numerical Optimization and Validation

Numerical optimization minimized both residual Fe and U+Th simultaneously. Table 5 presents the optimal conditions. The optimized solid-to-liquid (S/L) ratio lies at the lower boundary of the experimental range, indicating that a higher concentration of sulfuric acid (i.e., lower S/L ratio) was more effective in reducing impurity levels. The optimized temperature of 291°C is close to the upper limit (300°C), suggesting that elevated temperatures enhance the removal of Fe and U + Th. Similarly, the optimized reaction time, which reached the upper limit of 120 minutes, implies that prolonged exposure to sulfuric acid at high temperatures promotes more effective dissolution and removal of these impurities [14].

Table 4. Numerical optimization results

Factor	Optimum Value
Temperature	291^{o}C
Time	120 minutes
S/L ratio	1.5
Fe (residual)	0.80 % (predicted)
U+Th (residual)	254 % (predicted)

To verify the reliability of the process conditions predicted by the RSM model, validation experiments were conducted in triplicate under the optimized conditions. The results are summarized in Table 6. The mean experimental residual Fe and U+Th were 0.82 ± 0.03% and 252±6 ppm, respectively. The close agreement between predicted and experimental values confirms model reliability [18].

Table 5. Validation of optimized conditions

Run	Fe % (experimental)	Fe % (Predicted)	Deviation (%)	U + Th (ppm) (experimental)	U+Th (ppm) (Predicted)	Deviation (%)
1	0.82	0.80	2.44	248	254	2.36
2	0.79	0.80	1.25	258	254	1.57
3	0.84	0.80	5.00	249	254	1.96
Mean ± SD	0.82 ± 0.03	-	2.90 ± 1.91	2.52 ± 6	-	1.96 ± 0.40

3.3 Characterization of the Acid-Baked Product

3.3.1 Chemical Composition and Compliance with Foundry Specifications

Table 7 presents the chemical composition of the acid-baked partially decomposed zircon sand in comparison with the specifications for foundry-grade zircon. The acid baking of the partially decomposed zircon with concentrated sulfuric acid under the optimized conditions significantly improved the quality of the zircon sand.

Table 7. Zircon Sand at Various Stages of Treatment

Oxide(%)	Partially Decomposed Sand	Acid Baked Sand	Foundry Limit [19]
Fe_2O_3	2.34	0.82	≤ 0.30
SiO_2	19.71	21.86	≤ 32.50
Al_2O_3	0.67	0.55	≤ 1.50
TiO_2	0.64	0.16	≤ 0.30
$ZrO_2 + HfO_2$	58.37	67.76	≥ 65.00
$U_3O_8 + ThO_2$	17200*	252*	< 500*
SnO_2	2.88	2.14	---
Na_2O	4.07	0.33	---
P_2O_5	0.19	0	---

**Parts per million (ppm)*

The Fe_2O_3 content decreased from 2.34% in the partially decomposed sand to 0.82% after sulfuric acid baking. The decrease in Fe_2O_3 content can be attributed to the formation of iron sulfates during baking [14]. The ferric sulfate produced is soluble in water and was removed during subsequent washing steps, which explains the reduction in Fe_2O_3 content after acid baking.However, it remains above the 0.30% foundry limit. Residual iron is likely associated with stable iron-bearing phases not readily attacked by concentrated sulfuric acid under the conditions employed. This is the primary limitation preventing complete foundry compliance. The slight increase in SiO_2 content in the acid baked sand is likely due to the selective removal of other impurities rather any form of reaction with sulfuric acid since silica is known to be inert to sulfuric acid. The SiO_2 concentration however, remained well below the maximum allowable limit of 32.50%. Similarly, SnO_2 content did not reduce significantly during treatment due to cassiterite being resistant to acid attack [20].The concentration of $ZrO_2 + HfO_2$ increased significantly from 58.37% in the partially decomposed sand to 67.76% in the

acid-baked sample exceeding the required minimum of 65%. These increases indicate that sulfuric acid baking treatment effectively removed significant non-zirconium impurities, resulting in a notable enrichment of zirconia content. The combined radionuclide concentrations were significantly reduced from 17,200 ppm to 252 ppm in the acid baked sand, through the formation of water-soluble thorium and uranium compounds [21, 22] that were washed from the treated zircon sands. Residual U+Th can be attributed to lattice-bound radionuclides within preserved metamict zircon [7, 9].

3.3.2 Mineral Phase Identification

The mineral phases were examined by XRD to complement the chemical analysis. Figure 3 shows the XRD pattern of the partially decomposed zircon sand. Figure 4 shows the XRD pattern of the partially decomposed sand after acid baking.

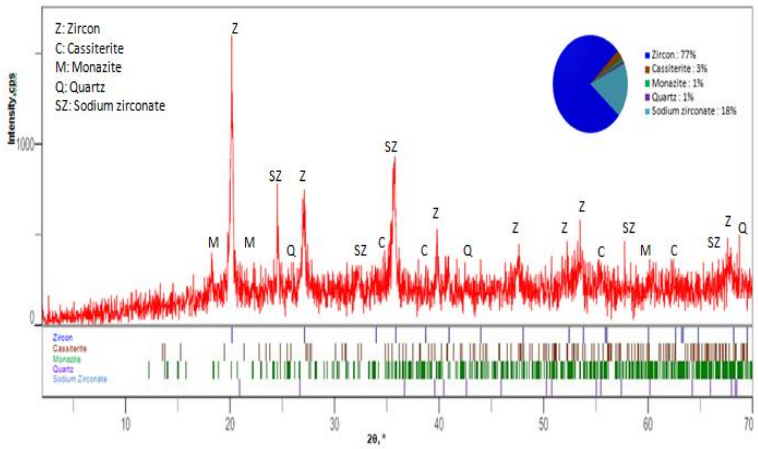

Figure 3. XRD pattern of the partially decomposed zircon sand

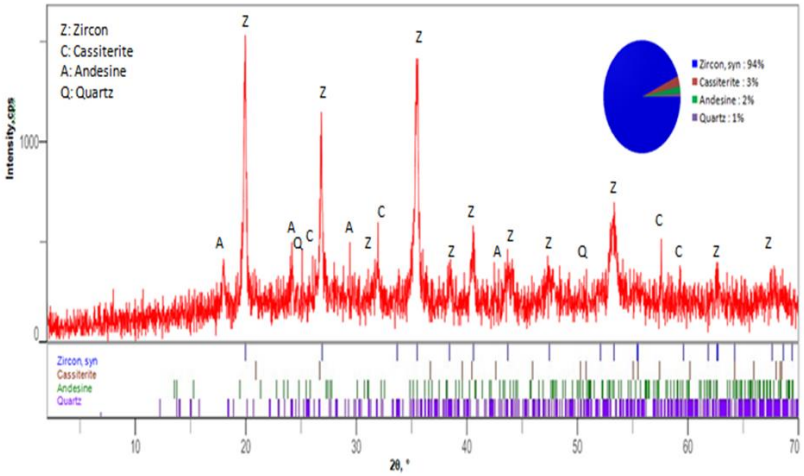

Figure 4. XRD pattern of acid baked zircon sand

The XRD analysis of the acid-baked partially decomposed zircon sand provided insight into the mineralogical transformations that occurred during the treatment process. The complete disappearance of sodium zirconate indicates that the acid baking stage effectively decomposed this phase, consistent with the known reaction of sodium zirconate with sulfuric acid to form soluble zirconium sulfate species [15] Similarly, the absence of monazite in the treated sample is attributed to its high susceptibility to sulfuric acid attack, resulting in its dissolution during acid baking and subsequent water leaching [22]. This observation is further supported by the elimination of P_2O_5 and the reduction in radioactive elements observed in the chemical composition of the treated sand (Table 7). Cassiterite, present at approximately 3 wt.%, remained essentially unaffected by the treatment, consistent with its well-documented resistance to both alkaline and acidic environments due to the high stability of its Sn–O bonds and its chemically inert tetragonal crystal structure [20]. Likewise, the persistence of quartz in minor quantities demonstrates its resistance to sulfuric acid under the

experimental conditions employed [10]. A minor amount (2 wt.%) of andesine (Ca, Na)(Al, Si)$_4$O$_8$, a sodium calcium aluminium silicate, was identified in the treated sample (Figure 4). Although its occurrence may be associated with mineralogical changes during the treatment process, the origin of this minor phase could not be established conclusively from the present study. Zircon remained the dominant mineral phase, accounting for approximately 94 wt.% of the treated sample. However, the persistence of cassiterite and quartz, together with the occurrence of minor secondary phases, limited the zircon content to below the minimum 97 wt.% required for foundry-grade zircon [19].

4 CONCLUSIONS

Acid baking of partially decomposed Riruwai zircon was successfully optimized using RSM-CCD. Optimal conditions were 291^{o}C, 120 min, and S/L = 1.5. Under these conditions, U+Th was reduced by 99% to 252 ppm, meeting the foundry radiological limit of <500 ppm. ZrO_2+HfO_2 increased to 67.76% (exceeding the 65% minimum). XRD confirmed 94% zircon with complete removal of sodium zirconate and monazite. Fe_2O_3 was reduced to 0.82% but remains above the 0.30% foundry limit.The overall process yields two valuable streams: a solid residue of treated zircon, and a liquid fraction of zirconium sulfate for ZrO_2 production. The process avoids fine milling, eliminating radioactive dust hazards. Future work should focus on iron removal via acid leaching, electrostatic separation for cassiterite, techno-economic assessment, and pilot-scale validation.

REFERENCES

1. Jain, P.L. (2009) Principles of Foundry Technology, (5th ed), *New Delhi: Tata McGraw-Hill*, pp. 83-90.
2. Dunan, C.F. (2019) Technical Handbook on Zirconium and Zirconium Compounds. *Zircon Industry Association*, pp. 29-40.
3. Pownceby, M.I., Sparrow, G.I., Aral, H., Smith, L.K. and Bruckard, W.J. (2015). Recovery and processing of zircon from Murray Basin mineral sand deposits. *Mineral Processing and Extractive Metallurgy*, vol. 124, no. 4. pp. 240-253.
4. Brown, J. (2000) (Ed) Foseco Ferrous Foundryman's Handbook. *Butterworth-Heinemann International*, pp. 150-156.
5. Okoli, B.I., Agboola, O.A., Onwualu, A.P., Bello, A., Sholiyi, O.S., Anye, V.C. and Yusuf, O.T. (2023). Characterization of Nigerian zircon sand and its suitability for different industrial applications. *Minerals*, vol. 13, no. 6, pp. 1-26.
6. Zambiri, S. (2009). Purification of some Nigerian zircon for use as opacifier using ammonium sulphate. *MSc thesis, Modibbo Adama University, Yola*, pp. 16-25.
7. Geisler, T., Pidgeon, R.T., van Bronswijk, W. and Kurtz, R. (2003). Transport of uranium, thorium, and lead in metamict zircon under low-temperature hydrothermal conditions. *Chemical Geology*, vol. 198, no. 4, pp. 293-307.
8. Smith, M.J., Jones, E., Blackburn, S. and Greenwood, R.W. (2023). Understanding the effect of metamictisation on the efficiency of zircon milling. *Minerals Engineering*, vol. 197, pp. 108065.
9. Aral, H., Sparrow, G.J., Mcdonald, K. and Norgate, T.E. (2007). Pure zircon process for removing radionuclides from zircon concentrates. *Transactions of the Institute of Mining andMetallurgy*, vol. 116, no. 3, pp. 145-151.
10. Barawy, K.A., El Tawil, S.Z. and Francis, A.A. (2000). Alkali fusion of zircon sand. *Mineral Processing and Extractive Metallurgy*, vol. 109, no. 1, pp. 49-56.
11. Subuki, I., Norsham, N.F.F., Mahayuddin, N.A. and Ali, Q.M. (2022). Influence on ratio of NaOH/$ZrSiO_4$ in alkali fusion for Amang zircon sand. *ASM Science Journal*, vol. 17, pp. 1-10.
12. Kefas, H.M., Chiroma, T.M., Patrick, D.O. and Mohammed, A. (2025). Optimization of Nigerian zircon sand partial decomposition using response surface methodology for foundry

applications. *Savannah Journal of Science and Engineering Technology*, vol. 3, no. (1), pp. 14-24.

13. Ledgerwood, J. and Van der Westhuyzen, P. (2011). The Use of Sulphuric Acid in the Mineral Sands Industry as a Chemical Mechanism for Iron Removal. *In: Proceedings of the 6th Southern African Base Metals Conference*, *Southern African Institute of Mining and Metallurgy*, pp. 169-180.
14. Dundas, R., (2018). Process for improving the grade and optical characteristics of zircon. *US Patent Application,* 2018/0127189 A1.
15. Da Silva, R.J.F., Dutra, A.J.B. and Afonso, J.C. (2012). Alkali fusion followed by a two-step leaching of a Brazilian zircon concentrate. *Hydrometallurgy*, vol. 117, pp. 93-100.
16. Gates-Rector, S.D. and Blanton, T.N. (2019). The powder diffraction file: a quality materials characterization database. *Powder Diffraction*, vol. 34, no. 4, pp. 352-360.
17. Hao, J., Wang, X., Wang, Y., Wu, Y. and Guo, F. (2022). Optimizing the leaching parameters and studying the kinetics of copper recovery from waste printed circuit boards. *ACS Omega*, vol. 7, no. 4, pp. 3689-3699.
18. Wang, X., Xiang, J., Pei, G., Li, L., Huang, Q. and Lv, X. (2021). Application of response surface methodology for roasting optimization in composite roasting—Acid leaching vanadium extraction process. *Chemical Engineering Research and Design*, vol.172, pp. 254-263.
19. Mohammed, A., Kareem, S.A. and Chiroma T.M. (2024). Chemical Beneficiation of Zircon Sand: A Review. *Savannah Journal of Science and Engineering Technology*, vol. 2, no. (4), pp. 133-141.
20. Tapster, S. and Bright, J.W.G. (2020). High-precision ID-TIMS cassiterite U-Pb systematic using a low-contamination hydrothermal decomposition. *Geochronology*, vol. 2, no. 2, pp. 425-441.
21. Berry, L., Galvin, J., Agarwal, V. and Safarzadeh, M. S. (2017). Alkali pug bake process for the decomposition of monazite concentrates. *Minerals Engineering*, vol. 109, pp. 32-41.
22. Helaly, O., Abdelmonem, N., El-Baky, K.A. and Ismail, I. (2021). Egyptian monazite digestion by sulphuric acid process; separation of thorium. *Water, Energy, Food and Environment Journal*, vol. 2, no. 1, pp. 35-49.